

WASI-2D: A software tool for regionally optimized analysis of imaging spectrometer data from deep and shallow waters



Peter Gege*

Deutsches Zentrum für Luft- und Raumfahrt (DLR), Earth Observation Center, Remote Sensing Technology Institute, Oberpfaffenhofen, 82234 Wessling, Germany

ARTICLE INFO

Article history:

Received 20 May 2013

Received in revised form

24 July 2013

Accepted 26 July 2013

Available online 6 August 2013

Keywords:

Remote sensing

Water

Inversion

Bio-optical models

Hyperspectral

ABSTRACT

An image processing software has been developed which allows quantitative analysis of multi- and hyperspectral data from oceanic, coastal and inland waters. It has been implemented into the Water Colour Simulator WASI, which is a tool for the simulation and analysis of optical properties and light field parameters of deep and shallow waters. The new module WASI-2D can import atmospherically corrected images from airborne sensors and satellite instruments in various data formats and units like remote sensing reflectance or radiance. It can be easily adapted by the user to different sensors and to optical properties of the studied area. Data analysis is done by inverse modelling using established analytical models. The bio-optical model of the water column accounts for gelbstoff (coloured dissolved organic matter, CDOM), detritus, and mixtures of up to 6 phytoplankton classes and 2 spectrally different types of suspended matter. The reflectance of the sea floor is treated as sum of up to 6 substrate types. An analytic model of downwelling irradiance allows wavelength dependent modelling of sun glint and sky glint at the water surface. The provided database covers the spectral range from 350 to 1000 nm in 1 nm intervals. It can be exchanged easily to represent the optical properties of water constituents, bottom types and the atmosphere of the studied area.

© 2013 The Author. Published by Elsevier Ltd. Open access under [CC BY-NC-ND license](http://creativecommons.org/licenses/by-nc-nd/4.0/).

1. Introduction

The water colour, or more precisely the water leaving spectral radiance, bears much information about the water body and possibly the bottom. Extraction of this information in optically complex waters, in which two or more components affect the colour, requires sensors that provide well-calibrated radiance spectra and so-called bio-optical models capable of simulating these spectra for all expected conditions. Data analysis is based on inversion of the bio-optical model, i.e. a number of model parameters are tuned such that the simulated spectra match the measured ones as good as possible. The derived model parameters are usually the concentrations of phytoplankton, dissolved organic matter and suspended sediments; in shallow waters additionally the water depth and coverage factors of bottom types like sand, macrophytes and phytobenthos.

Although many algorithms for inverse modelling of water leaving radiance and reflectance exist (IOCCG, 2006; Dekker

et al., 2011), no publicly available software was available for long time that can be regionally optimized by the user. The first software of this kind, BOMBER, was developed only recently (Giardino et al., 2012). It implements the remote sensing reflectance model of Lee et al. (1998, 1999) to generate maps of water constituents and, in case of shallow waters, maps of bottom depth and three substrate classes. A similar tool is presented in this paper, WASI-2D. It is based on the Water Colour Simulator WASI (Gege, 2004; Gege and Albert, 2006), which has been developed to simulate and analyse different types of spectral measurements of instruments disposed above the water surface and submerged in the water. An overview of the model options and software features, and a comparison with BOMBER, is given in Table 1.

Both tools were originally developed for application in lakes, but due to their general design they can be used in other aquatic environments as well, e.g. the open ocean, coastal zones or estuaries. While BOMBER is based entirely on a model of remote sensing reflectance, WASI-2D includes also a model of downwelling irradiance. It enables WASI-2D to correct the wavelength dependent reflections of the sun disk and the sky at the water surface (sun glint, sky glint), and it allows to process, besides reflectance, also upwelling radiance data. As WASI-2D can handle mixtures of up to 6 classes of phytoplankton, it can be used for phytoplankton classification, which is not feasible with BOMBER. WASI-2D is operated under Microsoft Windows as standalone

* Tel.: +49 8153 281242.

E-mail address: peter.gege@dlr.de

Table 1

Overview of major features of WASI-2D and comparison with BOMBER.

Bio-optical model	WASI-2D	BOMBER
Reference	Albert and Mobley (2003), Albert (2004)	Lee et al. (1998, 1999)
Spectrum type	<ul style="list-style-type: none"> Remote sensing reflectance Upwelling radiance 	Remote sensing reflectance
No. of phytoplankton classes	6	1
No. of bottom substrate types	6	3
Specific absorption of phytoplankton	From files	From file; can be related to chlorophyll concentration
Specific absorption of gelbstoff	<ul style="list-style-type: none"> Exponential function; slope can be fit parameter From file 	Exponential function; slope can be related to gelbstoff absorption
Specific absorption of non-algal particles	From file	Exponential function; slope can be fit parameter
Specific backscattering of suspended matter	<ul style="list-style-type: none"> Power law; exponent can be fit parameter From file; can be related to suspended matter concentration 	From file
Specific backscattering of phytoplankton	From file; can be related to chlorophyll concentration	From file
Artefacts	Sun glint, sky glint	Constant offset
Software implementation		
Software environment	Windows	ENVI+IDL
Programming language	Delphi 7.0	IDL
Image format description	<ul style="list-style-type: none"> ENVI header Manual input in menu ENVI header From ASCII files 	ENVI header
Sensor band description	Selectable band of image	ENVI header
Land mask	Downhill Simplex	Separate file
Inversion algorithm	Weighted least squares	CONSTRAINED_MIN based on generalized reduced gradient method
Residual	Least squares	Least squares
No. of fit parameters	<ul style="list-style-type: none"> Deep water: 21 Shallow water: 28 	<ul style="list-style-type: none"> Deep water: 4 Shallow water: 7
Fit quality measure	Residual and number of iterations	Relative error of reflectance
Test run of inversion	<ul style="list-style-type: none"> Single pixel Selected area 	Single pixel

program, while BOMBER is an add-on to the commercial ENVI image processing software, which requires fee-based licenses of IDL and ENVI. WASI-2D provides more options than BOMBER to fine-tune the inversion algorithm, e.g. calculation of standard deviation of selected image areas to determine the information-bearing bands, and wavelength-dependent weighting at residual calculation.

WASI-2D has been implemented as a new module into WASI. It can make use of all its spectrum types and bio-optical models and extends its functionality towards image processing. For remote sensing, upwelling radiance and remote sensing reflectance are the most relevant spectrum types. WASI includes a number of bio-optical models found in literature. The most general one is that of Albert (2004), Albert and Mobley (2003), Albert and Gege (2006), which can be applied to both optically deep and shallow waters. In Section 2 the equations of this model are recalled for the standard settings; a complete documentation of all implemented models and options is given in the user manual. The program features of WASI are described in Gege (2004, 2012), Gege and Albert (2006) and in the user manual. Useful capabilities of WASI for optimizing the operation of WASI-2D are the following. The *forward mode* can be used to determine the information bearing wavelength ranges by simulating measurements for the expected parameter ranges. The *single spectrum inverse mode* can be applied to in situ measurements of reflectance, irradiance, absorption or attenuation to determine optical properties and concentrations of water constituents, bottom reflectance and parameters of the atmosphere. The *reconstruction mode* allows sensitivity analysis and can be helpful to determine which parameters to fit and which to keep constant during inverse modelling.

2. Model

The quantity measured by an imaging sensor on board a satellite or aircraft is the at-sensor spectral radiance. It originates only partly from the water; a large portion comes from the atmosphere. WASI-2D does not model the influence of the atmosphere, thus the sensor data need to be corrected first for the atmospheric influences using a suitable software like ATCOR (Richter et al., 2006) or 6S (Vermote et al., 1997). Since the output of such software can be in units of spectral reflectance or spectral radiance, WASI-2D supports reflectance as well as radiance data. Conversion makes use of the relationship

$$L_u(\lambda) = R_{rs}(\lambda) \times E_d(\lambda). \quad (1)$$

This equation defines the remote sensing reflectance, R_{rs} , as the ratio of upwelling radiance, L_u , and downwelling irradiance, E_d . λ denotes wavelength. $E_d(\lambda)$ is calculated just above or below the water surface using the model of Gregg and Carder (1990); for details of the E_d model and its implementation in WASI see Gege (2012).

In the general case of optically shallow waters, L_u and R_{rs} are a sum of the contributions from the water surface, the water body and the bottom. Optically shallow means that L_u and R_{rs} are significantly affected by the bottom. A perfectly plane water surface acts like a mirror and reflects a well-defined section of the upper hemisphere, defined by the sky radiance L_s , into the sensor. The reflectance factor for L_s , ρ_{Ls} , is calculated as a function of the viewing angle, θ_v , using the Fresnel equation for unpolarized

light (Jerlov, 1976):

$$\rho_{Ls} = \frac{1}{2} \left| \frac{\sin^2(\theta_v - \theta'_v)}{\sin^2(\theta_v + \theta'_v)} + \frac{\tan^2(\theta_v - \theta'_v)}{\tan^2(\theta_v + \theta'_v)} \right|. \quad (2)$$

θ'_v is the angle of refraction, which is related to θ_v by Snell's law $n_W \sin \theta'_v = \sin \theta_v$, where $n_W \approx 1.33$ is the refractive index of water. For viewing angles near nadir, $\rho_{Ls} \approx 0.02$.

The water surface is almost never perfectly flat. Waves, ripples and foam create a complex surface structure, hence the reflected L_s is composed of radiation originating from different unknown locations of the sky, depending on the orientation of the wave facets within the pixels' field of view. For this reason WASI models L_s as a weighted sum of three light sources of known spectral irradiance:

$$L_s(\lambda) = g_{dd} \times E_{dd}(\lambda) + g_{dsr} \times E_{dsr}(\lambda) + g_{dsa} \times E_{dsa}(\lambda). \quad (3)$$

$E_{dd}(\lambda)$ represents the sun disk, $E_{dsr}(\lambda)$ Rayleigh scattering, and $E_{dsa}(\lambda)$ aerosol scattering. Their parameterization, which is adopted from the model of Gregg and Carder (1990), is described in Gege (2012). The weights g_{dd} , g_{dsr} and g_{dsa} represent the actual intensity of each light source for an image pixel and can be treated as fit parameters during data analysis. The remote sensing reflectance of the water surface is given by:

$$R_{rs}^{surf}(\lambda) = \rho_{Ls} \times \frac{L_s(\lambda)}{E_d(\lambda)}. \quad (4)$$

The contributions of the water body and the bottom to the reflected radiance are calculated for a hypothetical underwater sensor using the model of Albert and Mobley (2003), Albert (2004):

$$R_{rs}^{sh}(\lambda) = R_{rs}^{deep-}(\lambda) \times [1 - A_{rs,1} \times \exp\{-(K_d(\lambda) + k_{uW}(\lambda)) \times Z_B\}] + A_{rs,2} \times R_{rs}^b(\lambda) \times \exp\{-(K_d(\lambda) + k_{uB}(\lambda)) \times Z_B\}. \quad (5)$$

The superscript *sh* indicates shallow water, *deep* deep water, *b* bottom, and the '−' symbol a measurement just below the water surface. The first term on the right-hand side is the contribution of a water layer of thickness Z_B , the second term of the bottom. The reflected light has passed the water column twice. The corresponding extinction is described by the attenuation coefficients K_d for downwelling irradiance, k_{uW} for upwelling radiance originating from the water layer, and k_{uB} for upwelling radiance from the bottom. The radiative transfer program Hydrolight (Mobley et al., 1993) has been used to determine the empirical constants $A_{rs,1} = 1.1576 \pm 0.0038$ and $A_{rs,2} = 1.0389 \pm 0.0014$ by altering the water constituents concentrations over two orders of magnitude (Albert and Mobley, 2003). The low uncertainties of $A_{rs,1}$ and $A_{rs,2}$ indicate that Eq. (5) is applicable to a wide variety of water types.

The remote sensing reflectance above the water surface is related to that below through the following equation:

$$R_{rs}^{sh}(\lambda) = \frac{(1 - \rho_{Ed})(1 - \rho_{Lu-})}{n_w^2} \times \frac{R_{rs}^{sh-}(\lambda)}{1 - \rho_{Eu-} \times Q \times R_{rs}^{sh-}(\lambda)} + R_{rs}^{surf}(\lambda). \quad (6)$$

ρ_{Ed} , ρ_{Eu-} and ρ_{Lu-} are the reflection factors of E_d , E_u^- and L_u^- at the water surface, respectively, and $Q = E_u^-/L_u^-$ is the anisotropy factor of upwelling radiance. They depend on geometry parameters like sun zenith angle, cloud distribution and scattering phase functions of aerosols and suspended matter. The defaults in WASI are $\rho_{Ed} = 0.03$ (Jerlov, 1976), $\rho_{Lu-} = 0.02$ (from Fresnel Eq. (2)), $\rho_{Eu-} = 0.54$ (Jerome et al., 1990), and $Q = 5$ sr (Kirk, 1983).

The remote sensing reflectance of deep water is calculated as follows:

$$R_{rs}^{deep-}(\lambda) = f_{rs}(\lambda) \times u(\lambda). \quad (7)$$

In this equation, the factor f_{rs} parameterises the viewing and illumination geometry in terms of the viewing angle in water, θ'_v ,

and the sun zenith angle in water, θ'_{sun} :

$$f_{rs}(\lambda) = 0.0512 \times (1 + 4.6659 \times u(\lambda) - 7.8387 \times u(\lambda)^2 + 5.4571 \times u(\lambda)^3) \times \left(1 + \frac{0.1098}{\cos \theta'_{sun}}\right) \times \left(1 + \frac{0.4021}{\cos \theta'_v}\right). \quad (8)$$

The empirical coefficients have been determined using 177472 Hydrolight simulations by altering θ'_{sun} and θ'_v from 0 to 45°, chlorophyll concentration from 0.5 to 100 mg m^{−3}, suspended matter concentration from 0.5 to 50 g m^{−3}, gelbstoff absorption at 440 nm from 0.05 to 5 m^{−1}, and wind speed from 0 to 30 m s^{−1} (Albert and Mobley, 2003). The function $u(\lambda)$ comprises the inherent optical properties (IOPs) of the water body:

$$u(\lambda) = \frac{b_b(\lambda)}{a(\lambda) + b_b(\lambda)}. \quad (9)$$

The IOPs of the water body are calculated as follows:

$$a(\lambda) = a_W(\lambda) + a_{ph}(\lambda) + a_Y(\lambda) + a_d(\lambda), \quad (10)$$

$$b_b(\lambda) = b_{b,W}(\lambda) + b_{b,X}(\lambda). \quad (11)$$

$a_W(\lambda)$ and $b_{b,W}(\lambda)$ are the absorption and backscattering coefficients of pure water, respectively. The default spectrum $a_W(\lambda)$ is a combination from different sources: 350–390 nm, interpolation between Quickenden and Irvin (1980) and Buiteveld et al. (1994); 391–787 nm, Buiteveld et al. (1994); 788–874 nm, own unpublished measurements on UV-treated pure water; 875–1000 nm, Palmer and Williams (1974). For $b_{b,W}(\lambda)$ the relation of Morel (1997) is used: $b_{b,W}(\lambda) = b_1(\lambda/500)^{-4.32}$ (λ in nm) with $b_1 = 0.00111$ m^{−1} for fresh water and $b_1 = 0.00144$ m^{−1} for oceanic water with a salinity of 35–38‰.

Four types of water constituents are considered: phytoplankton, gelbstoff, detritus and suspended particles. The first three are parameterized by their spectral absorption coefficients $a_{ph}(\lambda)$, $a_Y(\lambda)$ and $a_d(\lambda)$, respectively; suspended particles by their spectral backscattering coefficient, $b_{b,X}(\lambda)$. Backscattering by phytoplankton is included in $b_{b,X}(\lambda)$.

Phytoplankton concentration is expressed as mass of the pigments chlorophyll-a plus phaeophytin-a per water volume (mg m^{−3}); its specific absorption coefficient is species dependent. Frequently, a mixture of several phytoplankton species is present in the water. The resulting phytoplankton absorption coefficient is the sum of the individual contributions:

$$a_{ph}(\lambda) = \sum C_i \times a_i^*(\lambda). \quad (12)$$

C_i is the concentration of phytoplankton class number i , $a_i^*(\lambda)$ is the specific absorption coefficient of that class. The WASI database provides 6 spectra $a_i^*(\lambda)$ representing the phytoplankton in lake Bodensee (Gege, 1998; Heege, 2000). Spectrum #0 represents a typical phytoplankton mixture in that lake, #1 cryptophyta with low concentration of the pigment phycoerythrin, #2 cryptophyta with high phycoerythrin concentration, #3 diatoms, #4 dinoflagellates, and #5 green algae.

Gelbstoff (yellow substance) is the coloured dissolved organic matter (CDOM) in the water and composed of a huge variety of organic molecules. Its absorption coefficient is calculated as $a_Y(\lambda) = Y a_Y^*(\lambda)$, where $a_Y^*(\lambda)$ is the specific absorption spectrum, normalized at a reference wavelength λ_0 , and $Y = a_Y(\lambda_0)$ is the absorption coefficient at λ_0 . The spectrum $a_Y^*(\lambda)$ can either be imported from file, or it can be modelled by the frequently used approximation $\exp[-S(\lambda - \lambda_0)]$. For the exponential approximation, $\lambda_0 = 440$ nm and $S = 0.014$ nm^{−1} are set by default, which is representative of a great variety of water types (Bricaud et al., 1981; Carder et al., 1989).

Detritus (also known as tripton (Gitelson et al., 2008) or bleached particles (Doerffer and Schiller, 2007)) is the collective

name for all absorbing non-algal particles in the water. Its absorption spectrum is parameterized as $a_d(\lambda) = Da_d^*(\lambda)$, with $a_d^*(\lambda)$ denoting specific absorption, normalized at the same wavelength λ_0 as Gelbstoff, and $D = a_d(\lambda_0)$ describing the absorption coefficient at λ_0 . The spectrum $a_d^*(\lambda)$ is imported from file.

Suspended particle concentration is expressed as dry mass per water volume (g m^{-3}). Its backscattering coefficient is calculated as

$$b_{bX}(\lambda) = X \times b_{bX}^* \times b_X(\lambda) + C_{Mie} \times b_{b,Mie}^* \times (\lambda/\lambda_S)^n \quad (13)$$

This equation allows to model mixtures of two spectrally different types of suspended matter. Type I is defined by a scattering coefficient with arbitrary wavelength dependency, $b_X(\lambda)$, which is imported from file. X is the concentration and b_{bX}^* the specific backscattering coefficient. b_{bX}^* can be treated as constant or as dependent on concentration, $b_{bX}^* = A \cdot X^B$. Such non-linear dependency with $A = 0.0006 \text{ m}^2 \text{ g}^{-1}$ and $B = -0.37$ was observed for open ocean waters, in which the concentrations of suspended matter and phytoplankton are highly correlated (Morel, 1980; Sathyendranath et al., 1989). For such waters, $X = C_0$ can be set in WASI, with C_0 denoting the concentration of phytoplankton class no. 0. Type II is defined by the normalized scattering coefficient $(\lambda/\lambda_S)^n$, where the Angström exponent n is related to the particle size distribution. C_{Mie} is the concentration and $b_{b,Mie}^*$ the specific backscattering coefficient. Default values are $b_{bX}^* = 0.0086 \text{ m}^2 \text{ g}^{-1}$, $b_X(\lambda) = 1$, $b_{b,Mie}^* = 0.0042 \text{ m}^2 \text{ g}^{-1}$, $\lambda_S = 500 \text{ nm}$, $n = -1$, which are representative for lake Bodensee (Heege, 2000).

The attenuation coefficients are calculated as follows (Albert (2004), Albert and Gege (2006)):

$$K_d(\lambda) = 1.0546 \times \frac{a(\lambda) + b_b(\lambda)}{\cos \theta'_{sun}}, \quad (14)$$

$$k_{uW}(\lambda) = \frac{a(\lambda) + b_b(\lambda)}{\cos \theta'_v} \times [1 + u(\lambda)]^{3.5421} \times \left[1 - \frac{0.2786}{\cos \theta'_{sun}} \right], \quad (15)$$

$$k_{uB}(\lambda) = \frac{a(\lambda) + b_b(\lambda)}{\cos \theta'_v} \times [1 + u(\lambda)]^{2.2658} \times \left[1 + \frac{0.0577}{\cos \theta'_{sun}} \right]. \quad (16)$$

Bottom reflectance is implemented for mixtures of up to six substrate types as

$$R_{rs}^b(\lambda) = \sum f_i \times B_i \times R_i^b(\lambda). \quad (17)$$

Each substrate type is characterized by an irradiance reflectance spectrum $R_i^b(\lambda)$. B_i is the fraction of radiation that is reflected in sensor direction if the bottom is covered to 100% by substrate type i ; $B_i = 1/\pi = 0.318 \text{ sr}^{-1}$ represents a Lambertian surface with isotropic reflection. f_i is the areal fraction of substrate type i within an image pixel; it is $\sum f_i = 1$. The WASI database provides 6 spectra $R_i^b(\lambda)$ from the German lakes Bodensee and Starnberger See (Pinnel, 2007). Spectrum #0 represents constant reflectance, #1 sand, #2 fine-grained sediment, #3 the green macrophyte *Chara contraria*, #4 the green macrophyte *Potamogeton perfoliatus*, and #5 the green macrophyte *Potamogeton pectinatus*.

3. Software implementation

WASI has been developed using Borland Delphi 7.0 for the operating system Microsoft Windows. The executable program including user manual can be downloaded from the IOCCG website (IOCCG, 2013a), the source code can be obtained from the author on request. The numerous model and program options are described in Gege (2004, 2012), Gege and Albert (2006) and in more detail in the manual. Here, mainly the new features relevant for processing of image data are described. The term 'WASI' is used for the complete software, while 'WASI-2D' refers specifically to the image processing module.

3.1. Graphical user interface

To illustrate the graphical user interface (GUI), a screenshot is presented in Fig. 1 which was made during inverse modelling of a hyperspectral image. The GUI consists in this case of two elements: an image preview window (Panel A), and the main WASI window known from the previous versions (Gege, 2004; Gege and Albert, 2006) (Panel B).

The image preview window opens automatically upon loading a hyperspectral image. It displays an RGB representation of the image using 3 selectable bands (3) and eventually a mask (4). During data analysis processed pixels get marked (2).

The components of the main WASI window are designated in the legend of Fig. 1. A major component is the parameter list (9). It comprises the potential fit parameters of all models implemented in WASI. Parameters irrelevant for the selected model are disabled, i.e. the corresponding symbol and value is displayed in grey, and the value cannot be edited. Checked parameters are treated as fit parameters during inverse modelling, the others as constants. The image specific settings are made in the popup window shown in Fig. 2, which is accessed from the menu bar (12) via 'Options—2D'.

To visualize a hyperspectral image, three bands are selected in the 'Preview image' panel which define the screen brightness for red, green and blue. Their radiometric dynamics is adjusted to the 8-bit screen resolution by multiplying each signal with $256C/M$, where C is the contrast and M the maximum signal of the unmasked pixels. If 'Scale bands together' is unchecked, M is calculated individually for the red, green and blue bands; otherwise, M is the maximum of the three bands.

A mask defines the pixels which are ignored during processing. It is selected in the popup window shown in Fig. 2 using the 'Mask' settings. Water is in general darker than land or clouds at wavelengths above 700 nm; hence an infrared band can be taken to define the mask.

The image is imported by selecting in the menu bar 'File—Load image'. The user can visualize the spectrum of any pixel by clicking with the mouse on the pixel of interest. By using the arrow keys to move the mouse pointer, the pixel-by-pixel variability can be studied. Mean and standard deviation of an area can be visualized by drawing with the mouse a rectangle. The extracted spectra are displayed in the plot window (no. 6 in Fig. 1) and can be saved as ASCII file. Inverse modelling can be applied to each spectrum extracted in this way. This feature is useful to determine initial values of fit parameters or to analyse selected pixels for which field data are available.

3.2. Data format

The format parameters relevant for hyperspectral image data are summarized in Table 2. They are specified in the 'Hyperspectral image' panel of the popup window shown in Fig. 2. WASI can alternately import the image parameters from an ENVI header file (ENVI, 2005), which is widely used as file format descriptor in the remote sensing community. The ENVI header file must be located in the same directory as the image and have the filename of the image with the extension '.hdr'.

WASI-2D supports as input five data types (8-bit byte, 16-bit unsigned integer, 16-bit signed integer, 32-bit signed long integer, 32-bit floating point) and two interleave types (BIL=band interleaved per line, BSQ=band sequential); output is 32-bit floating point BIL or BSQ. Wavelengths are expressed in units of nm. If the ENVI header file uses other units for wavelength, the 'wavelength scale factor' specifies the conversion factor (e.g. 1000 if the units are μm). The 'intensity scale factor' can be used to re-scale all data by division with the specified value; when set to 1, no re-scaling is performed. Band dependent scaling is not supported.

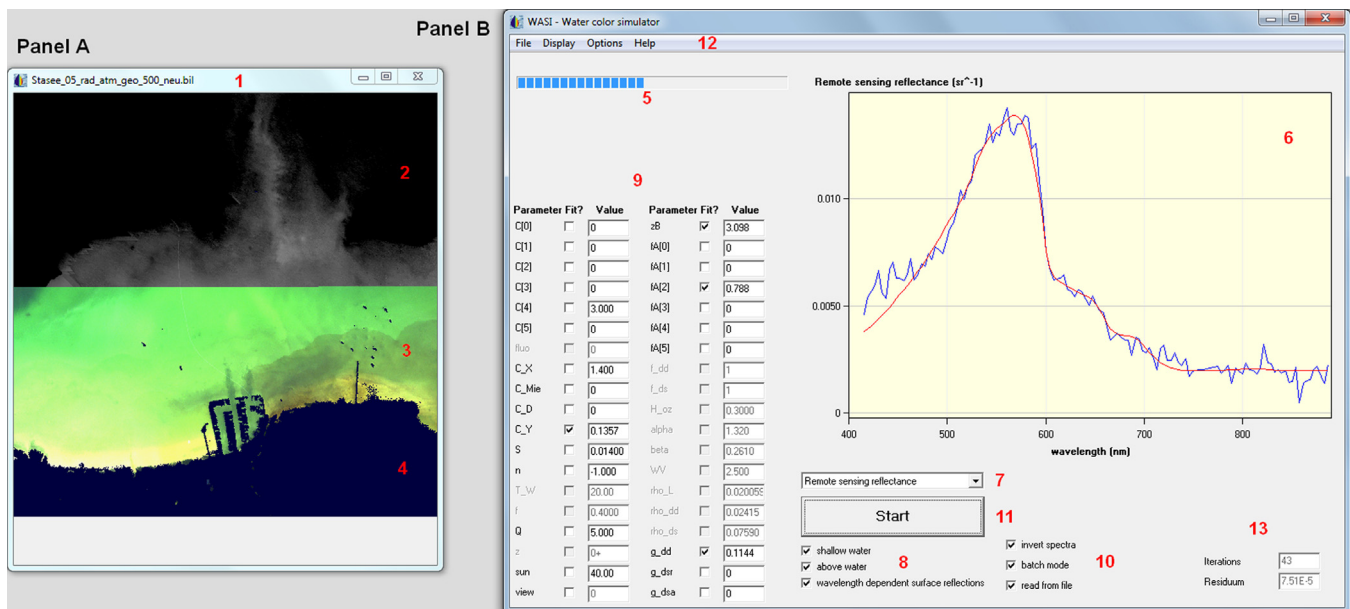


Fig. 1. Graphical user interface. Panel A: Image Preview of 2D-Module, Panel B: Main Window of WASI. (1) File name of image; (2) Processed pixels; (3) Original image; (4) Masked pixels; (5) Progress bar; (6) Spectrum of actually processed pixel (blue: measurement, red: fit curve); (7) Spectrum type; (8) Model options; (9) Parameter list; (10) Operation mode; (11) Start button; (12) Menu bar and (13) Fit quality measure. (For interpretation of the references to color in this figure legend, the reader is referred to the web version of this article.)

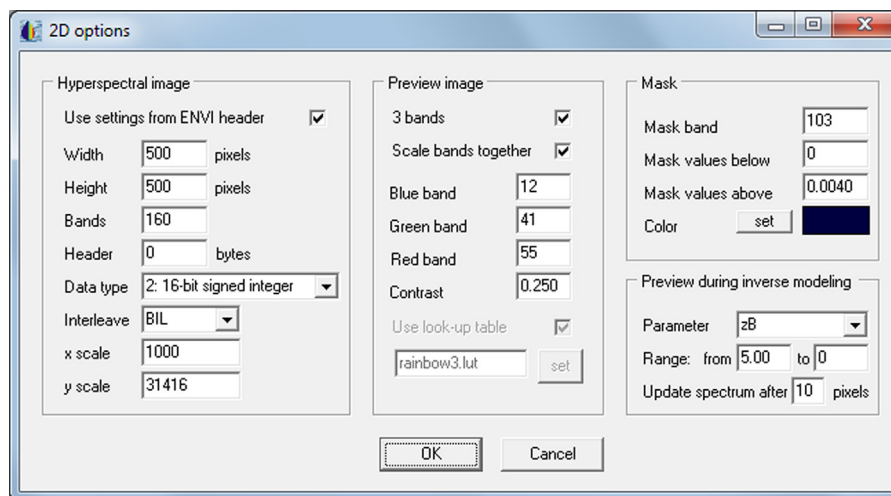


Fig. 2. Popup window for the options of WASI-2D.

3.3. Spectral resampling

The data files provided with WASI cover the spectral range from 350 to 1000 nm and have a spectral sampling interval of 1 nm. The user can exchange the files without limitations concerning range and sampling interval, but the number of data points is limited to 1300. To adjust the model curves to the sensor bands, the input data can be spectrally resampled to the centre wavelengths using Gaussian functions as weights. If this option is not used, the values closest to the centre wavelengths are taken for calculation. It is suggested to activate resampling unless the sensor bandwidth is less than 2 times the spectral library's data interval.

3.4. Inverse modelling

Inverse modelling of a measurement $M(\lambda)$ aims to determine the values of unknown model parameters $p=(p_1, p_2, \dots)$, called fit parameters. The parameters of the described bio-optical model are

Table 2
Image parameters.

Image parameter	WASI name	ENVI header keyword
Number of pixels per line	Width	samples
Number of image lines	Height	lines
Number of bands	Bands	bands
Centre wavelength of each band	(any ASCII table)	wavelength
Spectral resolution (FWHM) of each band	(any ASCII table)	fwhm
Image header offset	Header	header offset
Image data type	Data type	data type
Image interleave type	Interleave	interleave
Bands used for image visualization	Blue band Green band Red band	default bands
Wavelength scale factor	x scale	–
Intensity scale factor	y scale	–

listed in Table 3. The values of the unknown parameters are determined iteratively for each image pixel as follows. In the first iteration, a simulated spectrum $S(\lambda)$ is calculated for initial values $p^0 = (p_1^0, p_2^0, \dots)$ of the fit parameters. If the image is in units of remote sensing reflectance, $S(\lambda)$ corresponds to $R_{rs}^{sh}(\lambda)$ and modelling is done using Eq. (6); if the units are radiance, $S(\lambda)$ corresponds to $L_w(\lambda)$ and Eq. (1) is used for simulation. The simulated spectrum is compared with the measurement through the residual $R = B^{-1} [\sum_b g(\lambda_b) |S(\lambda_b) - M(\lambda_b)|^2]^{1/2}$ as a measure of correspondence. The coefficients $g(\lambda_b)$ allow for wavelength dependent weighting; the summation index b denotes the band number and B the number of bands. Then, in the further iterations, the p values are altered using the Downhill Simplex algorithm (Nelder and Mead, 1965; Caceci and Cacheris, 1984), resulting in altered model curves and altered residuals. The procedure is stopped when the calculated and the measured spectrum agree as good as possible, which corresponds to the minimum of R . The p values of the final step after N iterations, $p^N = (p_1^N, p_2^N, \dots)$, are the fit results.

3.5. Regional optimization

A number of model parameters can change regionally or seasonally, in particular the inherent optical properties of water constituents [$a_i^*(\lambda)$, $a_y^*(\lambda)$, $a_D^*(\lambda)$, $b_X(\lambda)$, $b_{b,X}^*$, $b_{b,Mie}^*$] and the apparent optical properties of the bottom [$R_i^b(\lambda)$, B_i] and the atmosphere. The database provided with WASI has been derived from in-situ measurements from lakes in Southern Germany (Gege, 1998; Heege, 2000; Pinnel, 2007). If no site-specific information is available, it can be used as a first approximation for other ecosystems as well. The variability within an ecosystem can be as large as between different ecosystem, i.e. ecosystem-specific sets of optical properties do not exist. However, region or season specific information should be used whenever available. Ideally, the optical properties should be measured at the test site close to the airplane or satellite overpass. This is however not always possible. A valuable source of information is the IOCCG webpage (IOCCG, 2013b). It maintains a list of links to publicly available data sets, for example the IOCCG (2006) data bank, the NASA bio-Optical Marine Algorithm Data set (NOMAD) and the SeaWiFS Bio-Optical Archive and Storage System (SeaBASS).

3.6. Fit parameter selection

Declaring a parameter as fit parameter or as constant is a critical step in data processing. The more parameters are fitted, the higher is the risk of failure due to ambiguous model curves. Furthermore, computation time increases with the number of fit parameters. Thus, the number of fit parameters should be chosen as low as justified by the variability within the scene. The more a parameter influences the spectral radiance or reflectance, the more important is an accurate estimate, and the more it should be considered as fit parameter in case it changes within the scene. Parameters with hardly changeable influence should be treated as constants.

The parameter list (9) of Fig. 1 summarizes all possible fit parameters of WASI. Most of them are usually treated as constants, and only a small fraction as fit parameters. A general rule cannot be given which parameters to fit and which to keep constant. An experience based suggestion is provided in Table 3 (column 'Fit?'). However, it cannot guarantee optimum results for each test site and at all conditions. If the results of data analysis are unsatisfactory, site-specific sensitivity analyses can be helpful to determine the appropriate fit parameters. The reconstruction mode of WASI has been developed for that purpose (Gege, 2004; Gege and Albert, 2006). It combines forward and inverse modelling and allows to introduce well-defined errors.

3.7. Fit parameter initialization

The success of inverse modelling depends on appropriate initialization of the fit parameters and their ranges. The start values are set in the parameter list of the main window (no. 9 in Fig. 1), the ranges in 'Options – Inverse calculation – Fit parameters'. Since the inversion algorithm sets the step sizes relative to the parameter values, the start value should not be set equal to zero to avoid trapping the parameter at zero.

In shallow waters, the influence of the bottom is modelled using Eq. (17) as a weighted sum of reflectance spectra $R_i^b(\lambda)$ representing the different substrate types within a pixel. The weights are the products of two parameters, f_i and B_i . f_i corresponds to the areal fraction of substrate no. i and can be

Table 3

Parameters of WASI-2D. 'Symbol' corresponds to the notation used in the text, 'WASI' to that in the software interface. 'Fit?' provides a suggestion when to use the parameter as fit parameter: x =in general, s =for shallow waters, $-$ =only exceptionally.

Symbol	WASI	Units	Fit?	Description
C_i	C[i]	mg m ⁻³	x^a	Concentration of phytoplankton class no. i , $i=0..5$
X	C_X	g m ⁻³	x	Concentration of suspended particles (type I)
C_{Mie}	C_Mie	g m ⁻³	$-$	Concentration of suspended particles (type II)
D	C_D	m ⁻¹	$-^b$	Concentration of detritus
Y	C_Y	m ⁻¹	x	Concentration of Gelbstoff
S	S	nm ⁻¹	x^c	Spectral slope of Gelbstoff absorption
n	n	$-$	$-$	Angström exponent of suspended particles (type II)
Q	Q	sr ⁻¹	$-$	Anisotropy factor of upwelling radiation
θ_{sun}	sun	deg	$-$	Sun zenith angle
z_B	zB	m	s	Water depth
f_i	fa[i]	$-$	s^d	Areal fraction of bottom surface type number i , $i=0.5$
H_{oz}	H_oz	cm	$-$	Scale height of ozone
α	alpha	$-$	$-$	Angström exponent of aerosols
β	beta	$-$	$-$	Turbidity coefficient
WV	WV	cm	$-$	Scale height of precipitable water in the atmosphere
g_{dd}	g_dd	sr ⁻¹	x	Fraction of sky radiance due to direct solar radiation (sun glint)
g_{dsr}	g_dsr	sr ⁻¹	$-$	Fraction of sky radiance due to molecule scattering (sky glint)
g_{dsa}	g_dsa	sr ⁻¹	$-$	Fraction of sky radiance due to aerosol scattering (sky glint)

^a Avoid too many classes; usually a single class is sufficient.

^b Fit D only if $a_D^*(\lambda)$ and $a_y^*(\lambda)$ are well-known and significantly different.

^c In Gelbstoff dominated water types.

^d Avoid too many types; usually three types are sufficient.

determined during inverse modelling if it is fit parameter. The 'BRDF parameter' B_i is the fraction of radiation that is reflected in sensor direction for $f_i=1$. Reflection is angle dependent for many substrate types, thus B_i can depend on the sun zenith angle, viewing direction and slope of the sea floor. As B_i is usually not well known and inverse modelling cannot distinguish between B_i and f_i , the identity $\sum f_i=1$ is often not useful. Thus, WASI assigns a lower and an upper limit to $\sum f_i$, representing in fact the range of $\pi \cdot \sum f_i B_i$. The range is set by default to 0.5–2.

3.8. Fit tuning

Inverse modelling of remote sensing data from water has frequently no unique solution since very different sets of model parameters can yield quite similar radiance and reflectance spectra (Defoin-Platel and Chami, 2007). Furthermore, sensor noise and inaccurate sensor calibration may cause wavelength-dependent errors of the measurements; atmosphere correction can introduce errors in the calculated water leaving radiance and reflectance spectra; the optical properties of the water constituents and the bottom substrates are usually not accurately known; the ever changing geometry of the water surface makes the reflections of the sun, the sky and of clouds unpredictable for pixel sizes in the order of tens of meters and below. Thus, automated algorithms cannot provide optimal results for all conditions.

For this reason WASI provides a number of options which enable users to fine-tune the inversion algorithm to known peculiarities of their dataset and to optimize processing for certain parameters of interest. The settings are made in a popup window (not shown) which is accessed from the menu bar via 'Options – Inverse calculation – Fit tuning'. A complete documentation is given in the user manual. Important settings are wavelength range and data interval of the calculated spectra, and the allowed maximum R_{max} of the residuum. The Downhill Simplex algorithm converges always towards a (local) minimum, but it can happen that no parameter set exists which produces a conveniently matching fit curve with a residuum smaller than R_{max} . To prevent the inversion algorithm from being trapped in an endless loop, an upper limit N_{max} of iterations is set; the default is $N_{max}=1000$. If data processing requires frequently N_{max} steps, the model parameters and R_{max} should be checked. The coefficients $g(\lambda_b)$, which are used for wavelength dependent weighting of the difference between measured and fit curve during residual calculation, are imported from file. The default file EINS.TXT, representing $g(\lambda_b)=1$, corresponds to the classical least squares fit.

3.9. Data processing

After the optical properties have been adapted to the test area, fit parameters have been chosen and initialized, and fit tuning options have been defined, data processing is started by pressing the 'Start' button (no. 11 in Fig. 1). A dialog requests to enter a filename for the fit results. The default extension of the output image is 'fit'. Processing starts with the first non-masked pixel top left and ends bottom right. The correspondence between model curves and measured spectra can be checked continuously in the plot window (no. 6 in Fig. 1), which displays both curves for each n th processed pixel. The interval n can be changed in the popup window shown in Fig. 2 ('Update spectrum after n pixels'). The progress can be tracked in the image preview window: processed pixels change their colour to grey. The shade of grey represents the result of a fit parameter as specified in the 'Preview during inverse modelling' box of the popup window shown in Fig. 2. Both features enable a first quality control already during data processing. The fit results are saved continuously to file during data processing, thus

stopping processing (using the 'Pause' button) conserves the results obtained so far.

The result of inverse modelling is a multi-band image in which the preceding bands correspond to the fit parameters and the last two to the residual (R) and the number of iterations (N), respectively. All program settings are documented automatically as ASCII file, and the image properties as ENVI header file to facilitate import by other software.

4. Summary

WASI-2D is a new image processing software for multi- and hyperspectral data from deep and shallow waters. It has been developed for inverse modelling of atmospherically corrected data from airborne sensors and satellite instruments and supports radiance as well as reflectance spectra. The executable program including user manual can be downloaded from the IOCCG website (IOCCG, 2013a), the source code can be obtained from the author on request. As WASI has been designed for accurate analysis of regional data by experienced users, but not for automated processing of large datasets covering a wide variety of optical properties, it is intended primarily for research and educational purposes, but not for commercial applications.

References

- Albert, A., Mobley, C.D., 2003. An analytical model for subsurface irradiance and remote sensing reflectance in deep and shallow case-2 waters. *Optics Express* 11, 2873–2890.
- Albert, A., 2004. Inversion Technique for Optical Remote Sensing in Shallow Water. Ph.D. Dissertation, Universität Hamburg, Hamburg, Germany, 188pp.
- Albert, A., Gege, P., 2006. Inversion of irradiance and remote sensing reflectance in shallow water between 400 and 800 nm for calculations of water and bottom properties. *Applied Optics* 45, 2331–2343.
- Bricaud, A., Morel, A., Prieur, L., 1981. Absorption by dissolved organic matter of the sea (yellow substance) in the UV and visible domains. *Limnology and Oceanography* 26, 43–53.
- Buiteveld, H., Hakvoort, J. H. M., Donze, M., 1994. The optical properties of pure water. In: *Proceedings SPIE 2258, Ocean Optics XII*, pp. 174–183.
- Caceci, M.S., Cacheris, W.P., 1984. Fitting curves to data. *Byte* 9, 340–362.
- Carder, K.L., Harvey, G.R., Ortner, P.B., 1989. Marine humic and fulvic acids: their effects on remote sensing of ocean chlorophyll. *Limnology and Oceanography* 34, 68–81.
- Defoin-Platel, M., Chami, M., 2007. How ambiguous is the inverse problem of ocean color in coastal waters? *Journal of Geophysical Research* 112, C03004, <http://dx.doi.org/10.1029/2006JC003847>.
- Dekker, A.G., Phinn, S.R., Anstee, J., Bissett, P., Brando, V.E., Casey, B., Fearn, P., Hedley, J., Klonowski, W., Lee, Z.P., Lynch, M., Lyons, M., Mobley, C., Roelfsema, C., 2011. Intercomparison of shallow water bathymetry, hydro-optics, and benthos mapping techniques in Australian and Caribbean coastal environments. *Limnology and Oceanography: Methods* 9, 396–425.
- Doerffer, R., Schiller, H., 2007. The MERIS Case 2 water algorithm. *International Journal of Remote Sensing* 28, 517–535.
- ENVI, 2005. ENVI User's Guide: ENVI Header Format, (http://geol.hu/data/online_help/ENVI_Header_Format.html), (accessed 19 May, 2013).
- Gege, P., 1998. Characterization of the phytoplankton in Lake Constance for classification by remote sensing. In: B  uerle, E., Gaedke, U. (Eds.), *Lake Constance—Characterisation of an Ecosystem in Transition*, 53. *Archiv f  r Hydrobiologie*, pp. 179–193.
- Gege, P., 2004. The water color simulator WASI: an integrating software tool for analysis and simulation of optical in situ spectra. *Computers & Geosciences* 30, 523–532.
- Gege, P., Albert, A., 2006. A tool for inverse modeling of spectral measurements in deep and shallow waters. In: Richardson, L.L., LeDrew, E.F. (Eds.), *Remote Sensing of Aquatic Coastal Ecosystem Processes: Science and Management Applications*. Springer, pp. 81–109.
- Gege, P., 2012. Analytic model for the direct and diffuse components of downwelling spectral irradiance in water. *Applied Optics* 51, 1407–1419.
- Giardino, C., Candiani, G., Bresciani, M., Lee, Z.P., Gagliano, S., Pepe, M., 2012. BOMBER: a tool for estimating water quality and bottom properties from remote sensing images. *Computers & Geosciences* 45, 313–318.
- Gitelson, A.A., Dall'Olmo, G., Moses, W., Rundquist, D.C., Barrow, T., Fisher, T.R., Gurlin, D., Holz, J., 2008. A simple semi-analytical model for remote estimation of chlorophyll-a in turbid waters: validation. *Remote Sensing of Environment* 112, 3582–3593.
- Gregg, W.W., Carder, K.L., 1990. A simple spectral solar irradiance model for cloudless maritime atmospheres. *Limnology and Oceanography* 35, 1657–1675.

- Heege, T., 2000. Flugzeuggestützte Fernerkundung von Wasserinhaltsstoffen am Bodensee. Ph.D. Dissertation. FU Berlin, Berlin, Germany. DLR-Forschungsbericht 2000-40, 134pp.
- IOCCG, 2006. Remote Sensing of Inherent Optical Properties: Fundamentals, Tests of Algorithms, and Applications. Lee, Z.P. (Ed.) Reports of the International Ocean-Colour Coordinating Group, No. 5. IOCCG, Dartmouth, Canada.
- IOCCG, 2013a. Software for Ocean-Colour Data, (<http://www.ioccg.org/data/software.html>) (accessed 19 May, 2013).
- IOCCG, 2013b. Supporting In-Situ Data, (<http://www.ioccg.org/data/insitu.html>) (accessed 19 May, 2013).
- Jerlov, N.G., 1976. Marine Optics. Elsevier Scientific Publishing Company, Amsterdam – Oxford – New York p. 231.
- Jerome, J.H., Bukata, R.P., Bruton, J.E., 1990. Determination of available subsurface light for photochemical and photobiological activity. *Journal of Great Lakes Research* 16 (3), 436–443.
- Kirk, J.T.O., 1983. Light and Photosynthesis in Aquatic Ecosystems. Cambridge University Press p. 401.
- Lee, Z.P., Carder, K.L., Mobley, C.D., Steward, R.G., Patch, J.S., 1998. Hyperspectral remote sensing for shallow waters: 1. A semianalytical model. *Applied Optics* 37, 6329–6338.
- Lee, Z.P., Carder, K.L., Mobley, C.D., Steward, R.G., Patch, J.S., 1999. Hyperspectral remote sensing for shallow waters: 2. Deriving bottom depths and water properties by optimization. *Applied Optics* 38, 3831–3843.
- Mobley, C.D., Gentili, B., Gordon, H.R., Jin, Z., Kattawar, G.W., Morel, A., Reinersman, P., Stamnes, K., Stavn, R., 1993. Comparison of numerical models for the computation of underwater light fields. *Applied Optics* 32, 7484–7504.
- Morel, A., 1980. In water and remote measurements of ocean colour. *Boundary-Layer Meteorology* 18, 177–201.
- Morel, A., 1997. Optical properties of pure water and pure Sea water. In: Jerlov, N.G., Steemann Nielsen, E. (Eds.), *Optical Aspects of Oceanography*. Academic Press, pp. 1–24.
- Nelder, J.A., Mead, R., 1965. A simplex method for function minimization. *Computer Journal* 7, 308–313.
- Palmer, K.F., Williams, D., 1974. Optical properties of water in the near infrared. *Journal of the Optical Society of America* 64, 1107–1110.
- Pinnel, N., 2007. A Method for Mapping Submerged Macrophytes in Lakes Using Hyperspectral Remote Sensing. Ph.D. Dissertation. TU München, Munich, Germany, 165pp.
- Quickenden, T.I., Irvin, J.A., 1980. The ultraviolet absorption spectrum of liquid water. *Journal of Chemical Physics* 72, 4416–4428.
- Richter, R., Schläpfer, D., Müller, A., 2006. An automatic atmospheric correction algorithm for visible/NIR imagery. *International Journal of Remote Sensing* 27, 2077–2085.
- Sathyendranath, S., Prieur, L., Morel, A., 1989. A three-component model of ocean colour and its application to remote sensing of phytoplankton pigments in coastal waters. *International Journal of Remote Sensing* 10, 1373–1394.
- Vermote, E.F., Tanré, D., Deuze, J.L., Herman, M., Morcrette, J.J., 1997. Second simulation of the satellite signal in the solar spectrum, 6 S: an overview. *IEEE Transactions on Geoscience and Remote Sensing* 35, 675–686.